

CWP-176
May 1995



**Anisotropy processing in vertically
inhomogeneous media**

Tariq Alkhalifah

Center for Wave Phenomena
Colorado School of Mines
Golden, Colorado 80401
303/273-3557

Anisotropy processing in vertically inhomogeneous media

Tariq Alkhalifah

ABSTRACT

Alkhalifah and Tsvankin (1995) show that P -wave normal-moveout (NMO) velocity for dipping reflectors in transversely isotropic (TI) media with a vertical symmetry axis, specified in terms of ray parameter, depends just on the zero-dip NMO velocity [$V_{\text{nmo}}(0)$], and a parameter η that is a combination of Thomsen's (1986) parameters. Their inversion procedure makes it possible to obtain η and reconstruct the NMO velocity as a function of ray parameter using moveout velocities for two different dips. Moreover, $V_{\text{nmo}}(0)$ and η determine not only the NMO velocity, but also long-spread (nonhyperbolic) P -wave moveout for horizontal reflectors and the time-migration impulse response. This means that inversion of dip-dependent information allows one to perform all time-processing in TI media using only surface P -wave data. Such findings have paved the way for constructing a full processing sequence for TI media.

The first and most important step in processing data in TI $v(z)$ media is parameter estimation. Alkhalifah and Tsvankin (1995) generalized the single-layer NMO equation to layered TI media with a dipping reflector. This equation provides the basis for extending TI velocity analysis to vertically inhomogeneous media. The multi-layered NMO equation is based on a root-mean-square (rms) average of modified interval velocities corresponding to a single ray parameter, that of the dipping event. Therefore, modified interval velocity values can be extracted from the stacking velocities using a Dix-type differentiation procedure. In addition, the η inversion is performed simultaneously with the interval velocity evaluation in each layer.

Since the moveout for reflections from steep reflectors is small and relatively insensitive to velocity, stacking-velocity estimates can be improved by applying velocity analysis after doing dip moveout correction (DMO), which increases the moveout, and therefore increases the moveout sensitivity to velocity. As a result, a modification to the NMO velocity equation is done to accommodate the application of the DMO operation, which here is based on the assumption of a homogeneous, isotropic medium.

Time migration, like DMO, depends on two parameters in vertically inhomogeneous media, namely the NMO velocity and η , both of which can vary with depth.

Therefore, the NMO velocity and η estimated using the dip dependency of P -wave moveout velocity can be used in a TI time migration.

An application of anisotropic processing to seismic data from offshore Africa demonstrates the importance of considering anisotropy, especially as it pertains to focusing dipping events.

INTRODUCTION

While it is convenient to consider the earth subsurface to be homogeneous, it is at a minimum vertically inhomogeneous. Through the combined action of gravity and sedimentation, velocity variation with depth represents the most important first-order inhomogeneity in the earth. This is one reason why time migration (based on lateral homogeneity) works well in so many places. Dip moveout (DMO) and migration algorithms that can handle isotropic $v(z)$ media are well established, and even velocity estimation in such media is considered trivial. Nevertheless, problems remain in focusing images, estimating depths, and preserving dipping events in $v(z)$ media. It may be that the problem at this point is the restrictive assumption that the medium is isotropic. Because basic processes that developed the earth's crust (i.e., sedimentation, pressure and gravity) have a preferred direction (vertical in most cases), seismic wave speed can vary with propagation direction in the vertical plane. Otherwise, it is difficult to explain the success of isotropic homogeneous DMO in areas with a clear velocity increase with depth (Gonzalez et al., 1992), knowing that such an increase in velocity causes the dipping events to stack at a lower velocity than the horizontal ones (Artley and Hale, 1994).

The first and most important step in a successful processing sequence for P -wave data is to estimate the medium parameters needed to apply the various processing operations. Existing work on anisotropic traveltimes inversion of reflection data has been done for laterally homogeneous subsurface models (Byun and Corrigan, 1990; Sena, 1991; Tsvankin and Thomsen, 1995). These inversions, although providing useful information on anisotropy in the subsurface, either use the weak-anisotropy approximation or require P -wave data to be supplemented by additional information (e.g., the vertical velocity from check shots or well logs). For example, the inversion method of Tsvankin and Thomsen (1995) requires acquisition of S -wave, as well as P -wave data, for estimation of anisotropy parameters to be feasible. One reason for the limitations associated with these algorithms is the number of parameters needed to be estimated in transversely isotropic (TI) media. Using Thomsen's (1986) notation, three parameters (V_{P0} , ϵ , and δ) are needed to characterize the kinematics of P -waves in TI media with vertical symmetry axis (VTI). As shown by Tsvankin and Thomsen (1995), P -wave moveout from horizontal reflectors is insufficient to recover the three Thomsen's parameters, even if long spreads (twice the reflector depth) are used. In fact, it is impossible to recover these three parameters using any additional surface P -wave data including moveout from dipping events (Alkhalifah and Tsvankin, 1995). The reason for this ambiguity is the trade-off between the

vertical velocity and anisotropic coefficients, which cannot be overcome by using any P -wave surface seismic information.

Therefore, there is a redundancy in the three-parameter representation that characterizes P -wave moveout in VTI media. In fact, Alkhalifah and Tsvankin (1995) demonstrated that, for TI media with vertical symmetry axis (VTI media), just *two* parameters are sufficient for performing all time-related processing such as NMO correction (including non-hyperbolic moveout correction, if necessary), DMO correction, and prestack and poststack time migration. Taking V_h to be the P -wave velocity in the horizontal direction, one of these two parameters, η , is given by

$$\eta \equiv 0.5 \left(\frac{V_h^2}{V_{\text{nmo}}^2(0)} - 1 \right) = \frac{\epsilon - \delta}{1 + 2\delta}, \quad (1)$$

and the other, the short-spread normal moveout (NMO) velocity for a horizontal reflector, is given by

$$V_{\text{nmo}}(0) = V_{P0} \sqrt{1 + 2\delta}, \quad (2)$$

where V_{P0} is the P -wave vertical velocity, and ϵ and δ are Thomsen's (1986) dimensionless anisotropy parameters.

These two parameters can also be characterized directly in terms of the elastic coefficients c_{ij} as follows

$$\eta = \frac{c_{11}(c_{33} - c_{44})}{2c_{13}(c_{13} + 2c_{44}) + 2c_{33}c_{44}} - \frac{1}{2},$$

and

$$V_{\text{nmo}}(0) = \sqrt{\frac{c_{13}(c_{13} + 2c_{44}) + c_{33}c_{44}}{(c_{33} - c_{44})}}.$$

The fact that we cannot uniquely determine the elastic coefficients from η and $V_{\text{nmo}}(0)$ does not matter, because time-related processing depends just on $V_{\text{nmo}}(0)$ and η .

Alkhalifah and Tsvankin (1995) further show that these two parameters, η and $V_{\text{nmo}}(0)$, can be obtained solely from surface seismic P -wave data, using estimates of stacking velocity for reflections from interfaces having two distinct dips.

The inversion technique discussed by Alkhalifah and Tsvankin (1995) is designed for a homogeneous medium above the reflector, while realistic subsurface models are, at a minimum, vertically inhomogeneous. Therefore, it is appropriate to extend the inversion mechanism of Alkhalifah and Tsvankin (1995) to handle vertically inhomogeneous media.

Alkhalifah (1995b) suggested to invert for η and $V_{\text{nmo}}(0)$ using the nonhyperbolic moveout behavior of P -wave reflections in vertically varying VTI media. Although this method does not require dipping events to be present, which makes it more flexible than the dip-dependent moveout approach of Alkhalifah and Tsvankin (1995), it is

less stable and depends on having reasonably large offsets to obtain realistic estimates of parameters at greater depths.

A key feature of time-related processing is that the final output is still given in time. Therefore, a reflection from a horizontal reflector at zero-offset (coincident source and receiver) remains in exactly the same position after applying NMO, DMO, and time migration. As a result, all transformations done by these processes are with respect to this zero-offset reflection rather than its depth position. This eliminates the need to specify the depth of the reflection point. In VTI media, such a feature is valuable because it eliminates the need for the vertical velocity when time-related processing are expressed in terms of $V_{\text{nmo}}(0)$ and η , and therefore, reduces the number of required parameters needed to specify these processes. (Vertical velocity, however, is required in any attempt to convert seismic data from time to depth.)

The bulk of the paper concentrates on the $v(z)$ inversion process. Here, I extend the inversion technique of Alkhalifah and Tsvankin (1995) to handle layered transversely isotropic media based on the fact that NMO velocity for dipping reflectors is a root-mean-square (rms) average of its interval values. Such an rms relation, derived by Alkhalifah and Tsvankin (1995) for transversely isotropic layered media, depends also on only $V_{\text{nmo}}(0)$ and η . Next, I study the dependence of both DMO and time migration on $V_{\text{nmo}}(0)$ and η in vertically inhomogeneous media. Then, I apply the inversion method, as well as anisotropy processing, to a marine data set from offshore Africa.

NMO VELOCITY FOR DIPPING REFLECTORS IN TI MEDIA

The analysis here is based on the equation for the normal-moveout (short-spread) velocity for dipping reflectors in a homogeneous anisotropic medium derived by Tsvankin (1995):

$$V_{\text{nmo}}(\phi) = \frac{V(\phi)}{\cos \phi} \frac{\sqrt{1 + \frac{1}{V(\phi)} \frac{d^2 V}{d\theta^2}}}{1 - \frac{\tan \phi}{V(\phi)} \frac{dV}{d\theta}}, \quad (3)$$

where V is the phase velocity as a function of the phase angle θ (θ is measured from vertical) and ϕ is the dip of the reflector; the derivatives are evaluated at the dip ϕ . Unfortunately, reflection data do not carry any explicit information about dip; rather, we can count on recovering the ray parameter $p(\phi)$ corresponding to the zero-offset reflection. Therefore, for inversion purposes, formula (3) must be recast in terms of the ray parameter (Alkhalifah and Tsvankin, 1995),

$$p(\phi) = \frac{1}{2} \frac{dt_0}{dx_0} = \frac{\sin \phi}{V(\phi)}, \quad (4)$$

where $t_0(x_0)$ is the two-way traveltime on the zero-offset (or stacked) section, and x_0 is the midpoint position. In this case, the phase angle ϕ and phase velocity $V(\phi)$

corresponding to a given value of p can be obtained from the Christoffel equation and used in formula (3) (Alkhalifah and Tsvankin, 1995).

VELOCITY ANALYSIS IN $V(Z)$ MEDIA

Inversion in layered VTI media can be implemented through a layer-stripping algorithm where the parameters of a certain layer (or interval) are estimated by removing the influence of the overlying layers. The layer-stripping portion of the inversion is similar to what Dix (1955) used to estimate interval velocities from stacking velocities based on a small-offset approximation.

NMO velocity equation for dipping reflectors in $v(z)$ media

For horizontal layers, whether the media are isotropic or VTI, the NMO velocity at a certain zero-offset time, t_0 , (equivalent to the migrated time, for horizontal layers) is given by an rms relation (Hake et al., 1984; Tsvankin and Thomsen, 1994) as follows

$$V_{\text{nmo}}^2(t_0) = \frac{1}{t_0} \int_0^{t_0} v_{\text{nmo}}^2(\tau) d\tau, \quad (5)$$

where $v_{\text{nmo}}(\tau)$ are “interval NMO velocities” given by

$$v_{\text{nmo}}(\tau) = v(\tau) \sqrt{1 + 2\delta(\tau)},$$

and $v(\tau)$ is the interval vertical velocity.

For dipping reflectors, when expressed in terms of ray parameter p , NMO velocity is also given by a similar rms relation (Alkhalifah and Tsvankin, 1995).

$$V_{\text{nmo}}^2[p, t_0(p)] = \frac{1}{t_0(p)} \int_0^{t_0(p)} v_{\text{nmo}}^2[p, t_m(\tau)] d\tau, \quad (6)$$

where $v_{\text{nmo}}[p, t_m]$ is the interval NMO velocity as a function of vertical time (migrated time), t_m , and $t_0(p)$ is zero-offset time for a single ray parameter, p . This ray parameter corresponds to the reflection from the dipping reflector at time $t_0(p)$ used to measure $V_{\text{nmo}}^2[p, t_0(p)]$, where $t_0(0) = t_m$ corresponds to the two-way traveltime to a horizontal reflector; i.e., migrated time. As demonstrated in equation (4), the ray parameter can be determined from the slope of the reflection in the zero-offset domain.

The integral in equation (6) can be expressed in terms of migrated time, t_m , as follows

$$V_{\text{nmo}}^2[p, t_0(p)] = \frac{1}{t_0(p)} \int_0^{t_m} v_{\text{nmo}}^2(p, \tau) \frac{dt_0(p)}{d\tau} d\tau. \quad (7)$$

This equation reduces to equation (5) for horizontal reflectors ($p = 0$), where $\frac{dt_0(p)}{d\tau} = 1$. Further, $v_{\text{nmo}}(p, \tau)$ depends only on the interval values $v_{\text{nmo}}(0, \tau)$ and $\eta(\tau)$ in each

layer or time sample. Alkhalifah and Tsvankin (1995) show that $t_0(p)$ is a function of the medium parameters $v_{\text{nmo}}(0)$ and η , as well as the vertical time, given by

$$t_0(p) = t_m f[\eta, v_{\text{nmo}}(0), p]. \quad (8)$$

Thus,

$$\frac{dt_0(p)}{dt_m} = f[\eta, v_{\text{nmo}}(0), p], \quad (9)$$

where f is the operator that relates the vertical time to the zero-offset time, which can be obtained through ray tracing. As a result, $V_{\text{nmo}}[p, t_0(p)]$ based on equation (7) depends on η and $v_{\text{nmo}}(0)$ in each layer. For isotropic media, $\eta = 0$, and

$$f[v_{\text{nmo}}(0), p] = \frac{1}{\sqrt{1 - p^2 v_{\text{nmo}}^2(0)}}.$$

Equation (6), when expressed in terms of discrete layers, is given by

$$[V_{\text{nmo}}^{(n)}(p)]^2 = \frac{1}{t_0(p)} \sum_{i=1}^n \Delta t_0^{(i)}(p) [v_{\text{nmo}}^{(i)}(p)]^2, \quad (10)$$

where $\Delta t_0^{(i)}(p)$ is the two-way zero-offset traveltimes through layer i for ray parameter p .

To obtain the NMO interval velocity in any layer i (including the one immediately above the reflector), we apply the Dix formula (Dix, 1955) to the NMO velocities at the top $[V_{\text{nmo}}^{(i-1)}]$ and bottom $[V_{\text{nmo}}^{(i)}]$ of the layer:

$$[v_{\text{nmo}}^{(i)}(p)]^2 = \frac{t_0^{(i)}(p)[V_{\text{nmo}}^{(i)}(p)]^2 - t_0^{(i-1)}(p)[V_{\text{nmo}}^{(i-1)}(p)]^2}{t_0^{(i)}(p) - t_0^{(i-1)}(p)}, \quad (11)$$

where $t_0^{(i-1)}(p)$ and $t_0^{(i)}(p)$ are the two-way traveltimes to the top and bottom of the layer, respectively, calculated along the ray given by the ray parameter p for normal-incidence reflection from the dipping reflector, used in measuring stacking velocity; all NMO velocities here correspond to a single ray-parameter value p . Suppose, we wish to use equation (11) to obtain the normal moveout velocity $[v_{\text{nmo}}^{(n)}(p)]$ in the medium immediately above the reflector to use as an input value in the inversion algorithm discussed above. Clearly, from equation (10), the recovery of $v_{\text{nmo}}^{(n)}(p)$ requires obtaining the moveout velocities in the overlying medium for the same value of the ray parameter. However, as we will see later, such a problem can be solved by using an interpolation procedure.

Inversion in $v(z)$ media

When interval NMO velocity values, $v_{\text{nmo}}^{(n)}(p)$, are obtained for at least two distinct dips, the problem reduces within each layer (or time sample, if the inversion was based

on the integral form) to a homogeneous inversion that can be solved in the same way described by Alkhalifah and Tsvankin (1995). Therefore, interval values $v_{\text{nmo}}^{(n)}(p)$ for two distinct dips in each layer (or each time sample) are used to estimate $\eta(\tau)$ and $v_{\text{nmo}}(0, \tau)$. Since estimating $v_{\text{nmo}}^{(n)}(p)$ using equation (11) depends on obtaining $v_{\text{nmo}}^{(i)}(p)$ for previous layers at the same ray parameter, estimating $\eta(\tau)$ and $v_{\text{nmo}}(0, \tau)$ must be done simultaneously with the layer-stripping process for $v_{\text{nmo}}^{(i)}(p)$.

First, I use the values $V_{\text{nmo}}^{(1)}(p_1)$ and $V_{\text{nmo}}^{(1)}(p_2)$, which correspond to the first interval, to estimate $\eta^{(1)}$ and $v_{\text{nmo}}^{(1)}(0)$ using the inversion of Alkhalifah and Tsvankin (1995) for a homogeneous medium, where p_1 and p_2 are ray parameters of the dipping reflectors in this first interval (one of these reflectors could be horizontal). Each interval is considered homogeneous. Then, I use the estimated $\eta^{(1)}$ and $v_{\text{nmo}}^{(1)}(0)$ to obtain $V_{\text{nmo}}^{(1)}(p_3)$ and $V_{\text{nmo}}^{(1)}(p_4)$, as well as $\frac{dt_0(p_3)}{dt_0}$ and $\frac{dt_0(p_4)}{dt_0}$, in the first interval. Ray parameters p_3 and p_4 correspond to the dipping (or horizontal) reflectors in the second interval. Using equation (11), I then obtain the interval values $v_{\text{nmo}}^{(2)}(p_3)$ and $v_{\text{nmo}}^{(2)}(p_4)$, which corresponds to the second interval, from $V_{\text{nmo}}^{(1)}(p_3)$ and $V_{\text{nmo}}^{(1)}(p_4)$, and in turn use them to obtain $\eta^{(2)}$ and $v_{\text{nmo}}^{(2)}(0)$, and so on.

Although the method requires NMO velocities measured at two different dips in each interval, one can define interval thicknesses depending on the available reflectors. Specifically, each interval is chosen to include two dips, no matter how large that interval gets. A better and more practical approach is to fit a piecewise-linear, continuous interval velocity models for each of the ray parameters of the dipping reflections used to measure the stacking velocities. These models satisfy these measured stacking velocities based on equation (7). Specifically, the interval velocities are taken as continuous at the times of the measured stacking velocities and linear in between. Eventually, we must obtain at least two continuous interval velocities corresponding to two distinct dips. As a result, the homogeneous inversion is applied at each time sample to obtain $v_{\text{nmo}}(0, \tau)$ and $\eta(\tau)$. A detailed description of the inversion is given in Appendix A.

As with isotropic media, intermediate interval values (i.e., values between measured ones) can be estimated using any interpolation technique between measured values. The sole requirement is that interval values yield the measured stacking velocities based on equation (7). For example, we could consider the measured values to be constant in each layer. Here, however, the application is based on a linear interpolation that keeps the inverted values continuous. This continuity is important for various ray tracing applications.

Errors in the inverted interval values of η can arise from the linear interpolation of velocities used in the layer-stripping process, and from the inversion in each homogeneous interval used to obtain η . The interpolation errors are similar to those encountered in layer-stripping applications for isotropic media. Errors associated with the homogeneous inversion, as described in detail by Alkhalifah and Tsvankin (1995), depend mainly on the accuracy of the measured quantities, primarily the stacking velocities.

Stacking-velocity measurements

As is well known, the stacking velocity for steep reflectors ($=\frac{V_{\text{nmo}}(0)}{\cos(\theta)}$ in isotropic homogeneous media, where θ is the reflector dip) is large; therefore, the moveout is small and insensitive to velocity. Specifically, the curvature of reflection moveout, dt^2/d^2X [$\propto 1/V_{\text{nmo}}^2$], where X is the source-receiver offset, decreases with increase in velocity. As a result, the resolution of velocity analyses is poor, causing problems in picking the appropriate stacking velocities corresponding to dipping reflectors.

One way to avoid this problem is to pick the stacking velocity after applying isotropic homogeneous DMO to the data. The DMO operation reduces the stacking velocity of dipping reflectors (approximately equivalent to multiplying by $\cos\theta$), and therefore, increases the sensitivity of moveout to velocity. As a result, I modify the NMO velocity equation in TI media to account for the isotropic homogeneous DMO operation. This is accomplished by including the traveltime shifts that correspond to the DMO operation in the NMO equation for dipping reflectors.

$$t^2(p, X) = t_0^2(p) + \left(\frac{1}{V_{\text{nmo}}^2(p)} + p^2\right)X^2 = t_0^2(p) + \frac{X^2}{V_{\text{stk}}^2(p)},$$

where t is the two-way traveltime as a function of offset, X . Therefore, the NMO velocity for a dipping reflector after isotropic homogeneous DMO is given by

$$V_{\text{stk}}(p) = \frac{V_{\text{nmo}}(p)}{\sqrt{1 + p^2 V_{\text{nmo}}^2(p)}}. \quad (12)$$

Equation (12) can, therefore, be used to replace the $V_{\text{nmo}}(p)$ function in inverting for η and $V_{\text{nmo}}(0)$.

There is an additional advantage in applying the DMO operation prior to velocity analysis in inverting for η . Specifically, we can verify the presence of anisotropy by comparing the NMO velocity of the sloping event (after DMO) to that of a horizontal event (or any other distinct slope). If the velocity of the sloping event is higher, then, in most cases, anisotropy is present, and η is positive. If the medium is also vertically inhomogeneous, then the anisotropy is even more significant, because inhomogeneity tends to reduce the influence of anisotropy on the isotropic homogeneous DMO operation (Alkhalifah, 1995a). If the velocity of the sloping event is lower than that of the horizontal event after applying a homogeneous isotropic DMO, then there are two possibilities: the first is that the medium is vertically inhomogeneous (Artley and Hale, 1994), and the second is that the medium is anisotropic with a negative η , which is unlikely (Thomsen, 1986; Alkhalifah and Tsvankin, 1995).

If the NMO velocities of the sloping and horizontal reflections are equal after applying homogeneous isotropic DMO (which is a goal of applying the DMO) then the medium may be isotropic and homogeneous, in concurrence with the type of operation used. However, if velocity analysis implies vertical inhomogeneity (which is typically the case), then anisotropy is present and has the same size (with an opposite

sign) influence as the vertical inhomogeneity on the DMO operation for these two dips (Gonzalez et al., 1992; Alkhalifah, 1995a). However, although the homogeneous isotropic DMO focussed these two reflections (the sloping and horizontal) at the same stacking velocity, it might not focus as well other reflections (with other slopes), because the isotropic $v(z)$ DMO impulse response is not identical to the anisotropic one (Alkhalifah, 1995a). Here, I have tried to outline the main possibilities. The presence of strong lateral inhomogeneity would introduce further complications.

TIME-RELATED PROCESSING

The main argument used to show the dependence of time-related processing (e.g., DMO and time migration) on only $V_{nmo}(0)$ and η in homogeneous VTI media is that such time-related processing become independent of the vertical velocity V_{P0} when expressed in terms of $V_{nmo}(0)$ and η . That is, it does not matter what values of V_{P0} , ϵ , and δ are used; only $V_{nmo}(0)$ and η need to be specified. To prove such an assertion, V_{P0} , ϵ and δ are varied from one test to another while keeping $V_{nmo}(0)$ and η the same, and changes in impulse responses (such as migration impulse responses or diffraction curves) are then observed. Alkhalifah and Tsvankin (1995) used such an argument for homogeneous media. Here I will apply it to vertically inhomogeneous media.

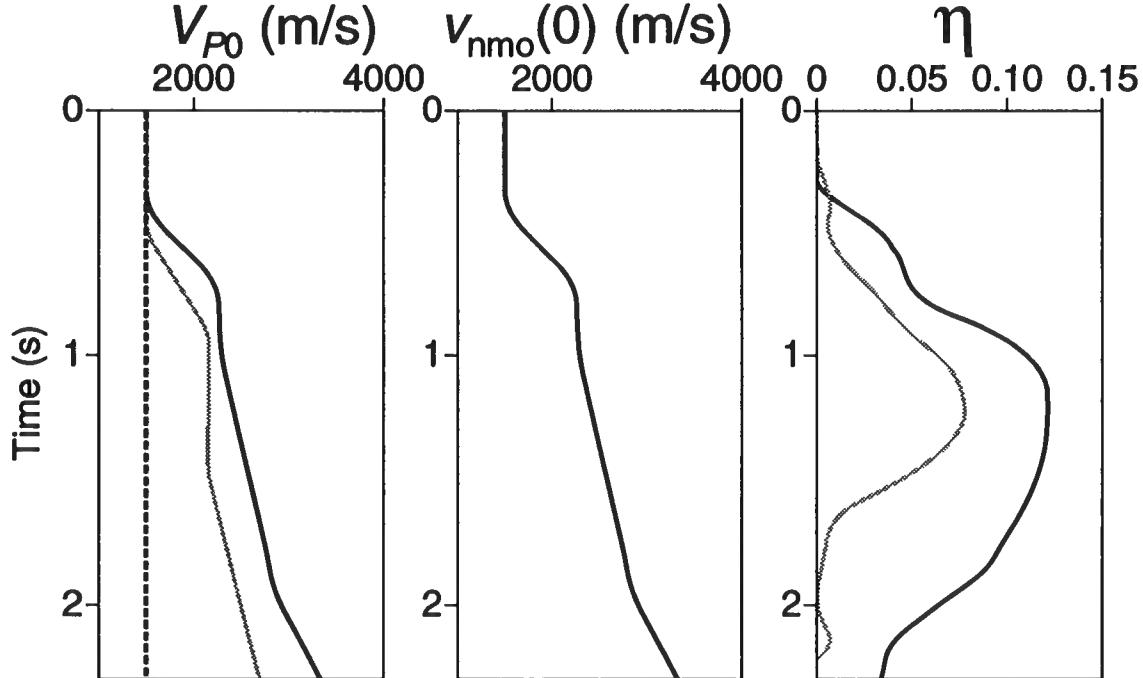


FIG. 1. Parameter variation as a function of vertical time. The parameters here correspond to the interval vertical velocity (V_{P0}), the interval NMO velocity for horizontal reflectors [$v_{nmo}(0)$], and the anisotropy parameter η . Different combinations of these parameters result in different models.

Figure 1 shows parameter variations as a function of vertical time that I use below to generate impulse responses. The vertical velocity (V_{P0}) given by the solid black curve is the same as the $v_{\text{nmo}}(0)$ curve, and, therefore, δ for this model equals zero. When combined with $v_{\text{nmo}}(0)$, the other two V_{P0} curves correspond to δ values that do not equal zero [see equation (2)]. The dashed curve (vertical velocity is a constant, 1500 m/s), when combined with $v_{\text{nmo}}(0)$, results in δ reaching values as large as the unrealistic value of 2. Therefore, in terms of Thomsen's (1986) parameters, the difference between the model given by the solid black V_{P0} curve and the model given the dashed curve is large, but the parameters have been chosen such that η is nevertheless the same.

Dip-moveout correction

As mentioned above, Alkhalifah and Tsvankin (1995) showed that the NMO velocity for dipping reflectors depends on only two medium parameters in homogeneous VTI media, namely $V_{\text{nmo}}(0)$ and η . Alkhalifah (1995a) further demonstrates that the DMO operation itself, as well as its impulse response, depends solely on these two parameters. This result holds as well for $\eta(\tau)$, as we see next.

Figure 2 shows four DMO impulse responses generated using the anisotropic DMO algorithm described by Alkhalifah (1995a). The first of these responses (Figure 2a) corresponds to the parameters given by the solid black curves in Figure 1 for V_{P0} , $v_{\text{nmo}}(0)$ and η . Note how different the DMO impulse response in VTI media are from the elliptical shape we have grown accustomed to for isotropic media. The responses in Figure 2b and 2c correspond to using the gray and the dashed curves of V_{P0} in Figure 1, respectively, while keeping the values of $v_{\text{nmo}}(0)$ and η the same as those used in Figure 2a (the solid black curves). The three DMO impulse responses look exactly the same; that is, they are independent of the value of V_{P0} , in support of the result that was partially suggested by equation (6), a small-offset approximation of the moveout. (Recall that for the response in Figure 2c, δ reaches values of about 2!) On the other hand, if we change η , using the gray curve in Figure 1 instead of the black one, the response changes dramatically, implying that it is highly dependent on η .

Time migration

Alkhalifah (1995b) showed that the nonhyperbolic moveout based on a Taylor's series expansion in vertically inhomogeneous VTI media is dependent on only $v_{\text{nmo}}(0, \tau)$ and $\eta(\tau)$. Again, such a moveout equation represents a small-dip approximation of a time-migration diffraction curve.

Figure 3 shows four time-migration impulse responses generated using an anisotropic phase-shift time migration (Kitchenside, 1991). The first of these responses (Figure 3a) corresponds to the parameters given by the solid black curves in Figure 1 for V_{P0} , $v_{\text{nmo}}(0)$ and η . On the other hand, the responses in Figure 3b and 3c correspond to using the gray and the dashed curves of vertical velocity (V_{P0}) from

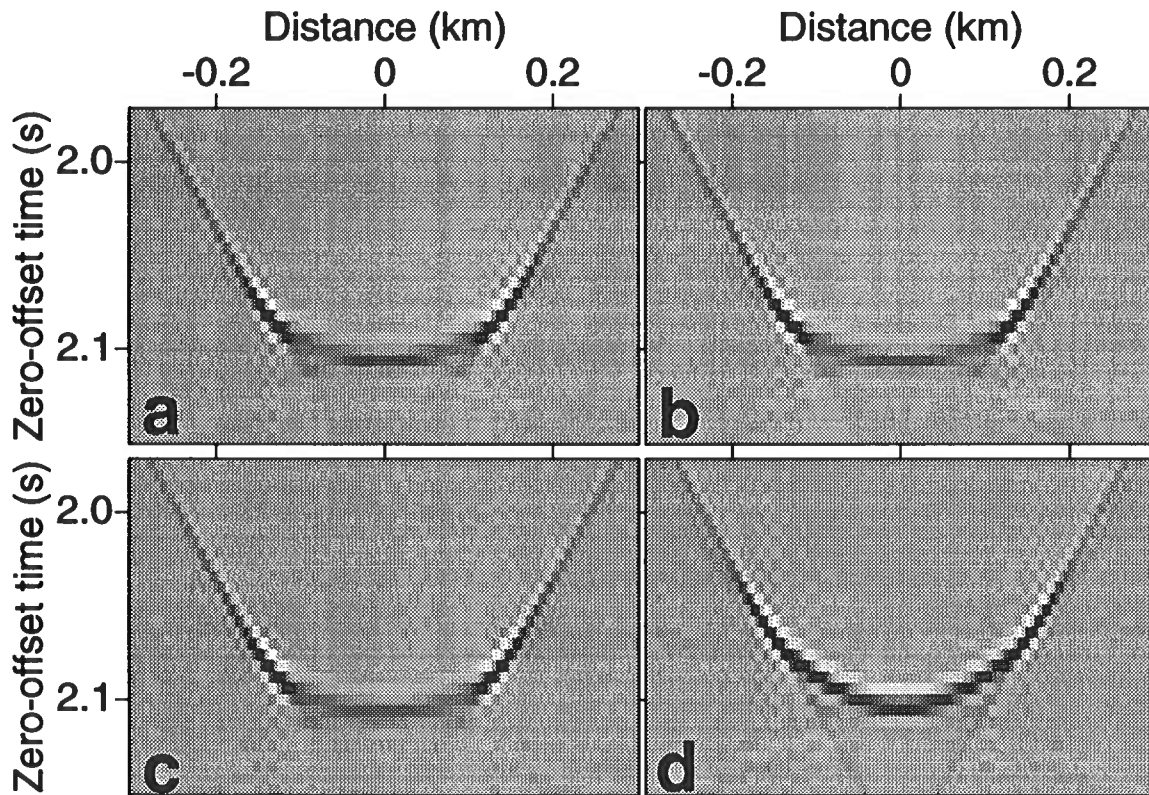


FIG. 2. DMO impulse responses for an impulse at time 2.1 s and offset 1.5 km using (a) the parameters represented by solid black curves in Figure 1, (b) the vertical velocity given by the gray curve in Figure 1 while keeping the other parameters the same as (a), (c) the vertical velocity given by the dashed curve in Figure 1 while keeping the other parameters the same as (a), and (d) the η values represented by the gray curve in Figure 1 while keeping V_{P0} and $v_{nmo}(0)$ the same as (a).

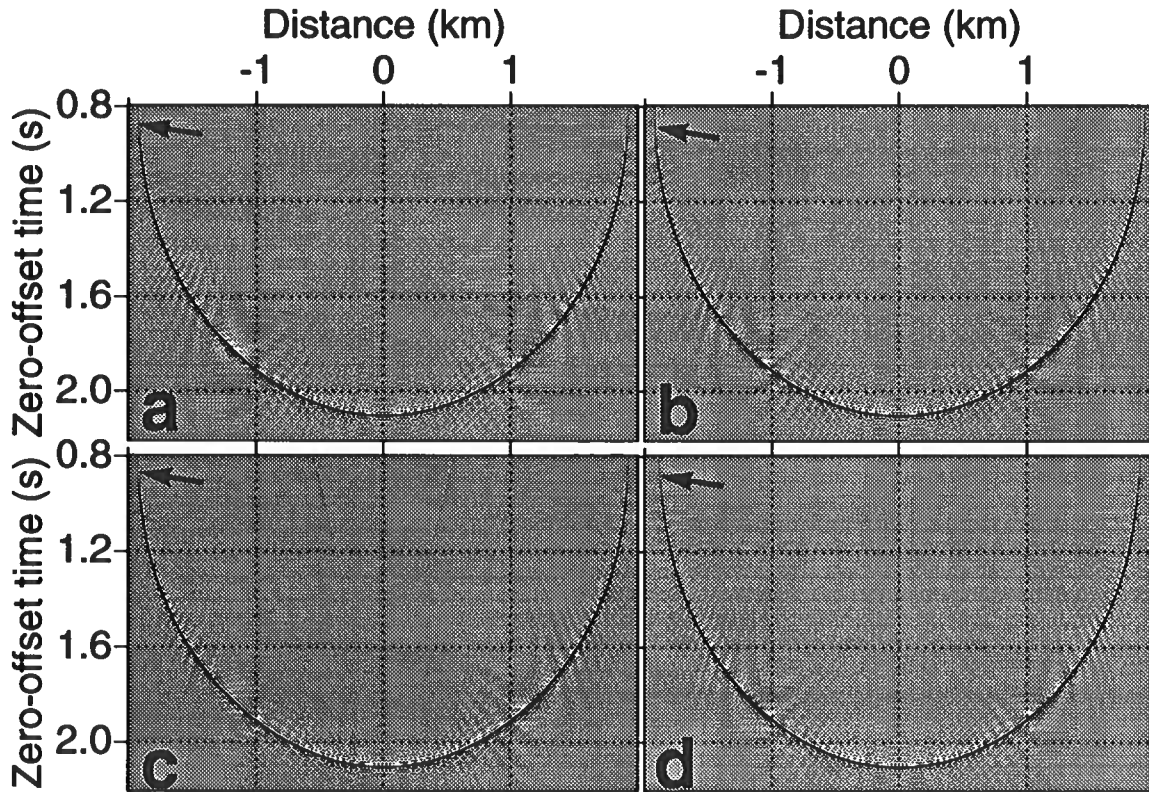


FIG. 3. Zero-offset time-migration impulse responses for an impulse at time 2.1 s, using (a) the parameters in Figure 1 represented by the solid black curves, (b) the vertical velocity given by the gray curve in Figure 1 while keeping the other parameters the same as (a), (c) the vertical velocity given by the dashed curve in Figure 1 while keeping the other parameters the same as (a), and (d) the η values represented by the gray curve in Figure 1 while keeping V_{P0} and $v_{nmo}(0)$ the same as (a).

Figure 1, respectively, while keeping $v_{\text{nmo}}(0)$ and η the same as those used in Figure 3a. The three time migration impulse responses look identical. Given the large difference between the Thomsen's parameters used to generate Figure 3a from those used to generate Figure 3c, the similarity of the responses that are based on the exact traveltime calculation (within the frame work of ray theory) is remarkable. Therefore, time migration in VTI media is also independent of vertical velocity when expressed in terms of $v_{\text{nmo}}(0)$ and η . However, if the gray η curve in Figure 1 is used, differences begin to appear. Specifically, note that, because of the overall lower η , the response in this case is slightly squeezed (see arrows). Although the time migration responses appear to have less variation with change in η than do the DMO responses, note that the scales at which the responses in the case of DMO and time migration are plotted are not the same. The conclusion in any event is that migration will be less sensitive to ignoring anisotropy than DMO, at least for modest dip. This is consistent with the results of Alkhalifah and Larner (1994).

FIELD-DATA EXAMPLE

Figure 4 shows a stacked seismic section, from offshore Africa provided by Chevron Overseas Petroleum, Inc., that contains reflections from a large number of dipping faults. The section was processed using a sequence of conventional NMO and DMO without taking anisotropy into account. While horizontal and mildly sloping reflections are imaged well, as we will see below, steep fault-plane reflections have been weakened because anisotropy was ignored. The predominant velocity variation in the section is vertical. In fact, in the area between CMP locations 400 and 800 and up to vertical time 3 s, the lateral variation of velocity is small.

The arrows in Figure 4 point to the sloping reflections used to measure the stacking velocities. Likewise, $V_{\text{nmo}}(0)$ measurements are based on the horizontal events. Although the sloping reflections used in the inversion seem to span the whole 5 s of data, the actual parameter information stops at about 3.5 s — the vertical (migrated) time corresponding to the deepest reflection used in the measurement of stacking velocity. This difference follows from the relation between the vertical time $[t_m]$ and the zero-offset time $[t_0(p)]$. In addition to the picked reflections, η at the surface is constrained to equal zero since these are marine data and the water layer is isotropic.

Carrying out the inversion process described in Appendix A, using the measured values of stacking velocities and corresponding ray parameters, I obtain the functions $v_{\text{nmo}}(\tau)$ and $\eta(\tau)$ shown in Figure 5. The inversion assumes no lateral velocity variation in the region of the picks; mild lateral velocity variation, however, should not be a problem for this DMO-based inversion: most DMO algorithms, while based on lateral homogeneity, still produce practical results where lateral velocity variation is smooth. The continuous representation shown in Figure 5 is a direct result of fitting a piecewise linear velocity model, as mentioned in Appendix A, for both the mildly dipping reflectors (for simplicity I refer to them as horizontal reflectors) and the faults. In the water layer, v_{nmo} is equal to 1.5 km/s and η , as mentioned earlier,

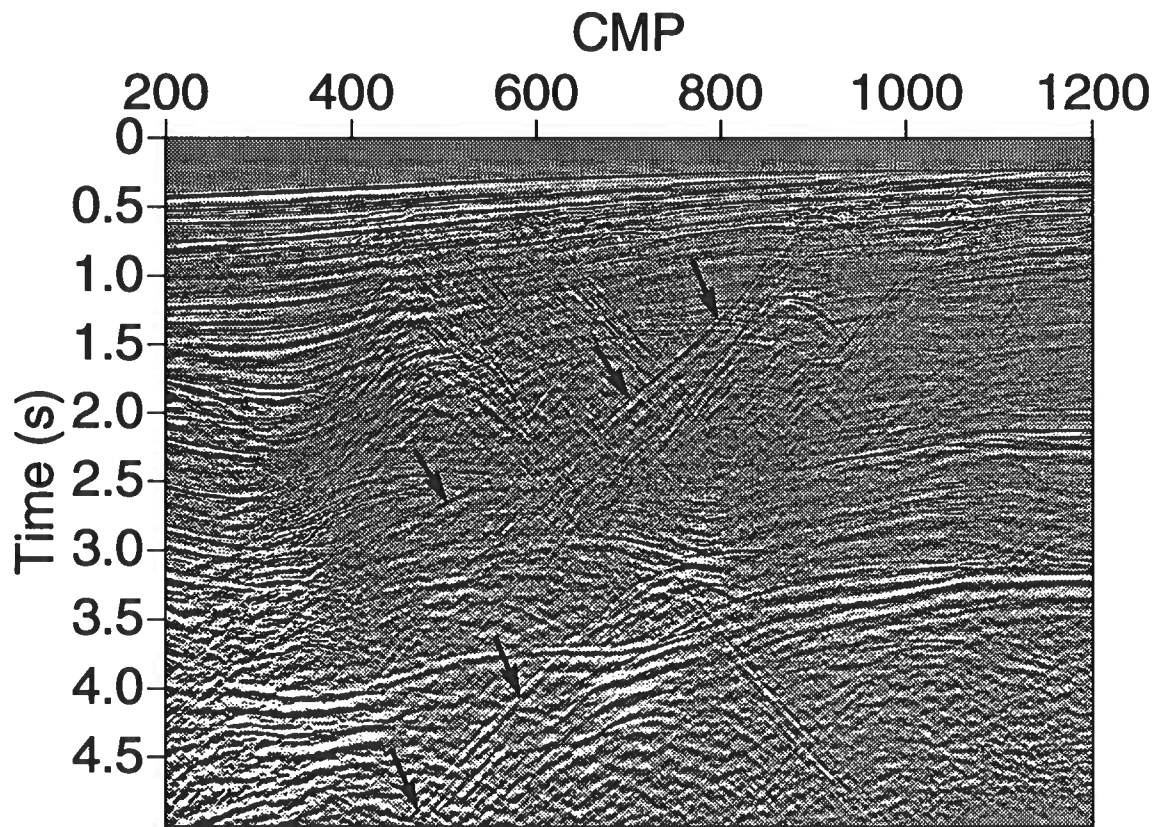


FIG. 4. Stacked section from offshore Africa, after applying NMO and isotropic homogeneous DMO. The arrows point to the sloping reflections used in the inversion.

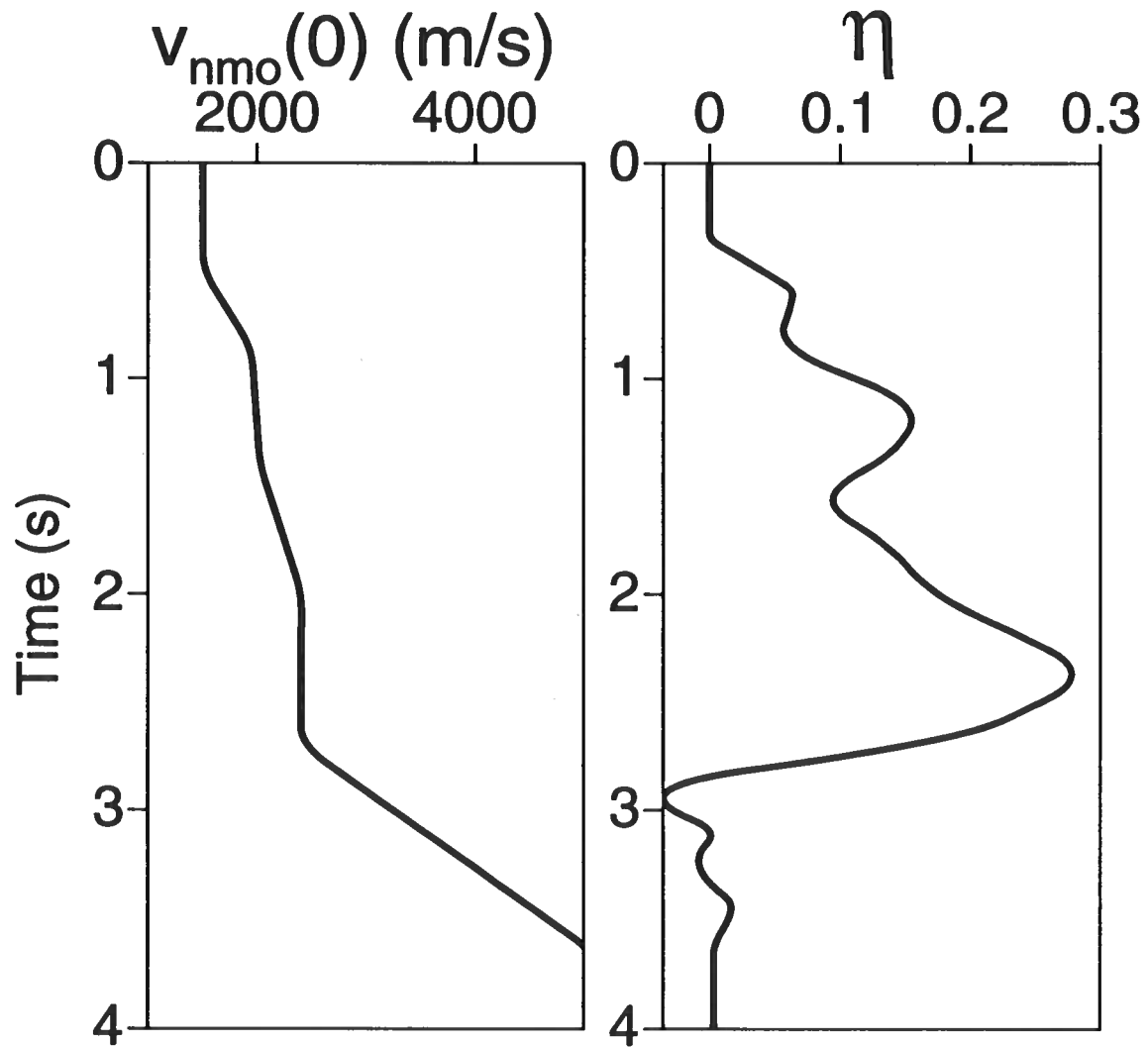


FIG. 5. Interval values v_{nmo} and η as a function of vertical time.

is equal to zero. The accuracy of these estimated curves of v_{nmo} and η depends on the accuracy of the stacking velocity estimates for both dipping and horizontal reflectors (Alkhalifah and Tsvankin, 1995). Based on the locations of the measured stacking velocities (Figure 4), as well as the extent of the lateral homogeneity, these inverted values can be considered representative of the area between CMP location 500 and 900.

The interval values of η in Figure 5 show more detail than can be reliably trusted considering the many uncertainties associated with the few events picked in these data and the particular assumption used for interpolating interval NMO velocities. However, we can still trust the general trend of the η curve, which implies an overall increase in the anisotropy with vertical time up to about 3 s. The η values after time equal 3.5 s were constrained to equal zero because no η information is present for these times using this inversion. The region above 3 s, which exhibits positive values of η , corresponds to a shale formation. Shale is often transversely isotropic and may thus be the major source of anisotropy in the data.

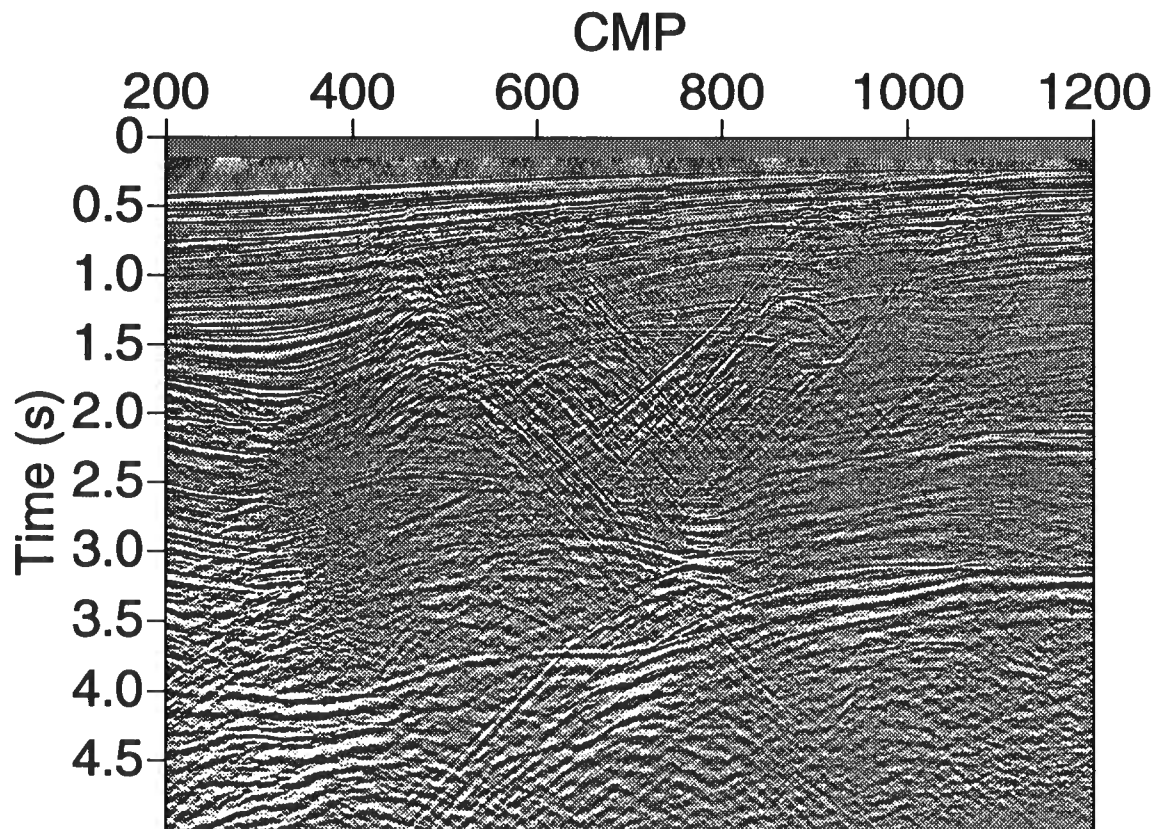


FIG. 6. Stacked section after $v(z)$ anisotropic DMO using the parameters in Figure 5. The NMO correction is based on the velocities obtained from the conventional velocity analysis. Compare with Figure 4.

Next, I apply a DMO algorithm that uses the derived functions $v_{\text{nmo}}(\tau)$ and $\eta(\tau)$ in Figure 5. Figure 6 shows the result of TI DMO applied to the data, based on the ray-

tracing DMO algorithm of Alkhalifah (1995a). Relative to the result of isotropic DMO given in Figure 4, this section is much improved. Note, in particular, the reflections from the faults. The improvements extend throughout the whole section, and includes reflections not used in the inversion. This implies that the lateral variation in η , especially prior to 2 s, is small.

Figure 7 shows representative VTI DMO operators used for these data. The shapes are far from the isotropic ellipse or even a stretched version of it. Therefore, we should expect the result from the anisotropic DMO to be different from that of the isotropic DMO, and so it is.

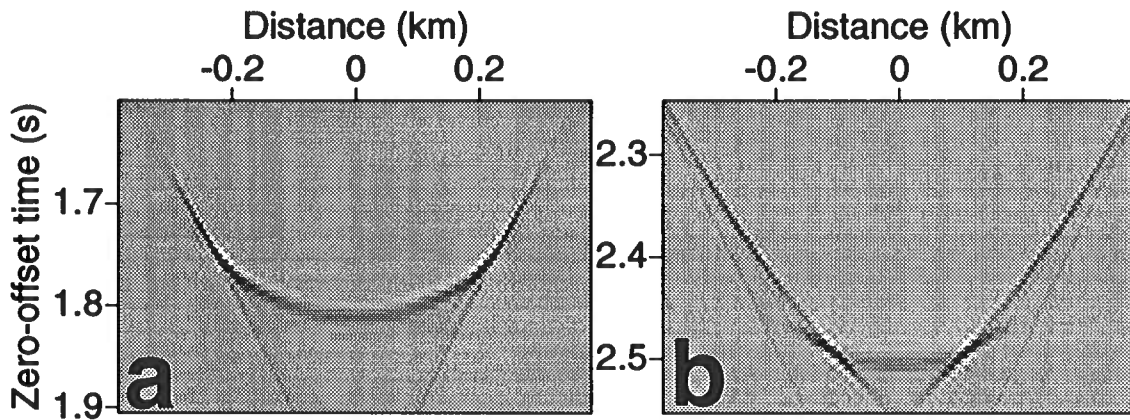


FIG. 7. VTI DMO impulses response for the parameters in Figure 5. The offset is 1.5 km, and the apex is at (a) 1.8 s, and (b) 2.5 s.

Figure 8 shows CMP gathers at CMP location 700 after (a) homogeneous isotropic DMO, and (b) $v(z)$ VTI DMO using the parameters in Figure 5. The same NMO correction, based on the stacking velocities obtained from conventional semblance velocity analysis, was used in both DMO examples. The arrows point to reflections from some of the dipping faults present in this highly faulted portion of the data. Note that the maximum offset is large (up to $X/D = 2$). Clearly, for the isotropic DMO result, the reflections from the dipping faults are not aligned. They have deviations caused by an NMO velocity that is smaller than what is needed for this anisotropic medium. Such deviations in reflection traveltimes are proportional to X^2 . Even the reflections from the horizontal events are not aligned. The misalignment for the horizontal reflections, however, is caused by the nonhyperbolic moveout associated with VTI media. Therefore, the deviations in this case start at larger offsets $X/D > 1$ (Tsvankin and Thomsen, 1994, Alkhalifah, 1995b), and are proportional to the nonhyperbolic term X^4 . This implies that the horizontal reflectors, as well as the dipping event, are less focused in Figure 4 than in Figure 6. Both horizontal and dipping events are better aligned after application of the ray-tracing anisotropic DMO based on the inverted parameters. Close comparison of Figures 4 and 6 reveals improvement in the horizontal features as a result of anisotropic processing.

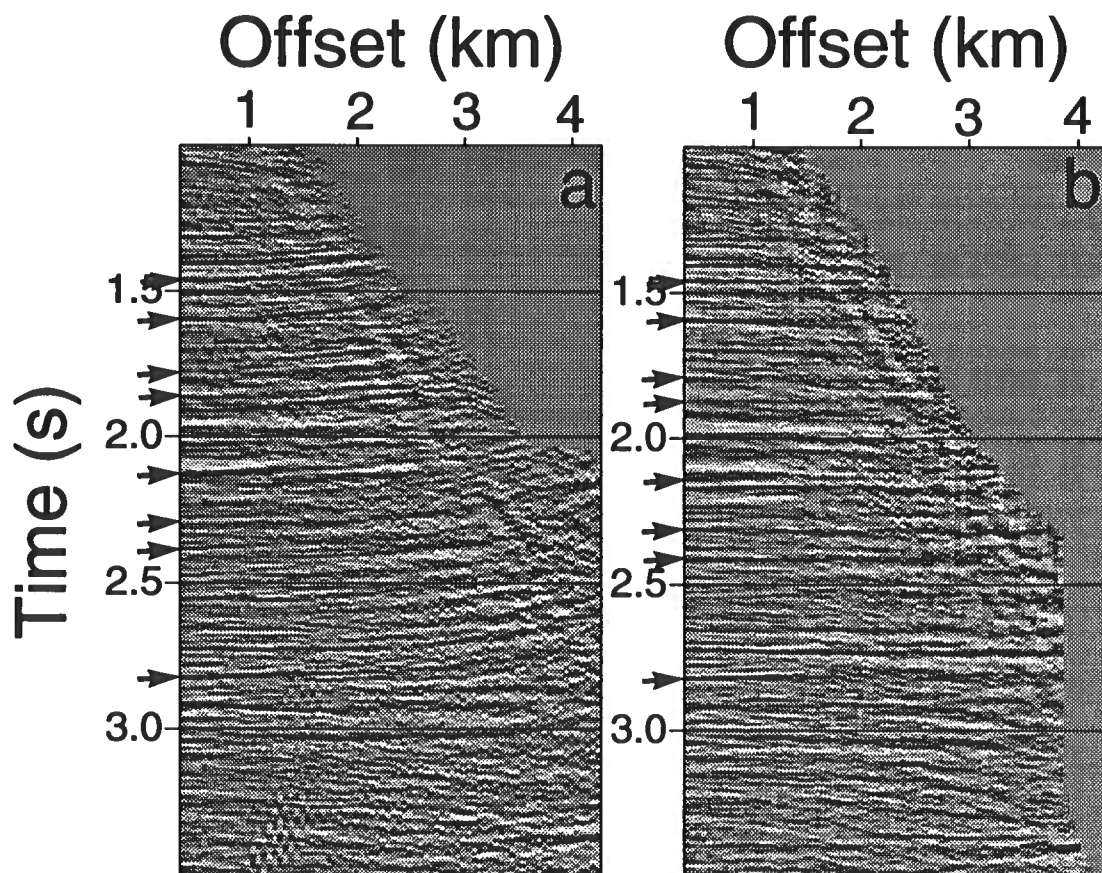


FIG. 8. CMP gathers for CMP location 700 after (a) homogeneous isotropic DMO, and (b) $v(z)$ anisotropic DMO. The NMO correction, based on the velocities obtained from velocity analysis, is the same for both examples.

Figure 9a shows the result of conventional processing: phase-shift, isotropic time migration was applied to the zero-offset section obtained by the isotropic homogeneous DMO. For comparison, Figure 9b shows the data imaged with phase-shift anisotropic time migration (using the inverted parameters of Figure 5) applied to the stack obtained from the $v(z)$ VTI DMO algorithm. This comparison gives a clear picture of the benefit of taking anisotropy into account in DMO prior to doing migration. The improvements here are numerous and significant. One example is the fault located at CMP location 870, between 2.5 and 3 seconds. An interpreter using the isotropic processing result can easily extend the reflections across this fault ignoring it or suggest a minor subsidence to the left of the fault. However, the imaged result of the anisotropic processing (as well as the inverted values of η) suggests the extension of the shales up to 3 seconds under CMP location 800, and probably a larger subsidence has occurred. Another example is the region of the nearly horizontal events near CMP location 500, at 2.5 s. The improved continuity of the gently dipping events likely is a result of non-hyperbolic moveout correction in the anisotropic processing.

Although most of the reflections here correspond to features within or near the 2-D plane that contains the sources and receivers, some events may represent out-of-plane reflections, requiring 3-D processing. Ignoring the three-dimensionality can cause mispositioning in some areas, especially where the fault reflections cross what seem to be continuous horizontal reflections. However, based on examination of parallel lines in the same area, most reflections are in the dip plane of the section.

Lynn et al. (1991) observe that problems of mis-focussing of dipping faults are encountered in many data sets from around the world and such problems can not be attributed to use of 2-D as opposed to 3-D processing, lateral velocity variations, or statics problems. Their assessment is that such problems are caused by the presence of anisotropy. They also state that isotropic prestack migration often gives poorer results than does isotropic poststack processing applied to DMO-processed data sets. Whereas full prestack migration seems to be the ideal way to process data, it is intolerant of any shortcomings of the model or the data.

DISCUSSION AND CONCLUSIONS

Although the inversion described here cannot resolve the vertical velocity and anisotropic coefficients ϵ and δ individually, it makes it possible to obtain the parameters needed to apply time-related processing (including NMO, DMO, and time migration) in vertically inhomogeneous media. These parameters are the zero-dip NMO velocity $v_{\text{nmo}}(0, \tau)$ and the anisotropy parameter $\eta(\tau)$.

The inversion algorithm described by Alkhalifah and Tsvankin (1995) was developed for a homogeneous, transversely isotropic medium above the reflector. To extend the method to vertically inhomogeneous media, the inversion must be applied using the NMO equation of Alkhalifah and Tsvankin (1995) for layered anisotropic media above a dipping reflector. The influence of a stratified isotropic or anisotropic

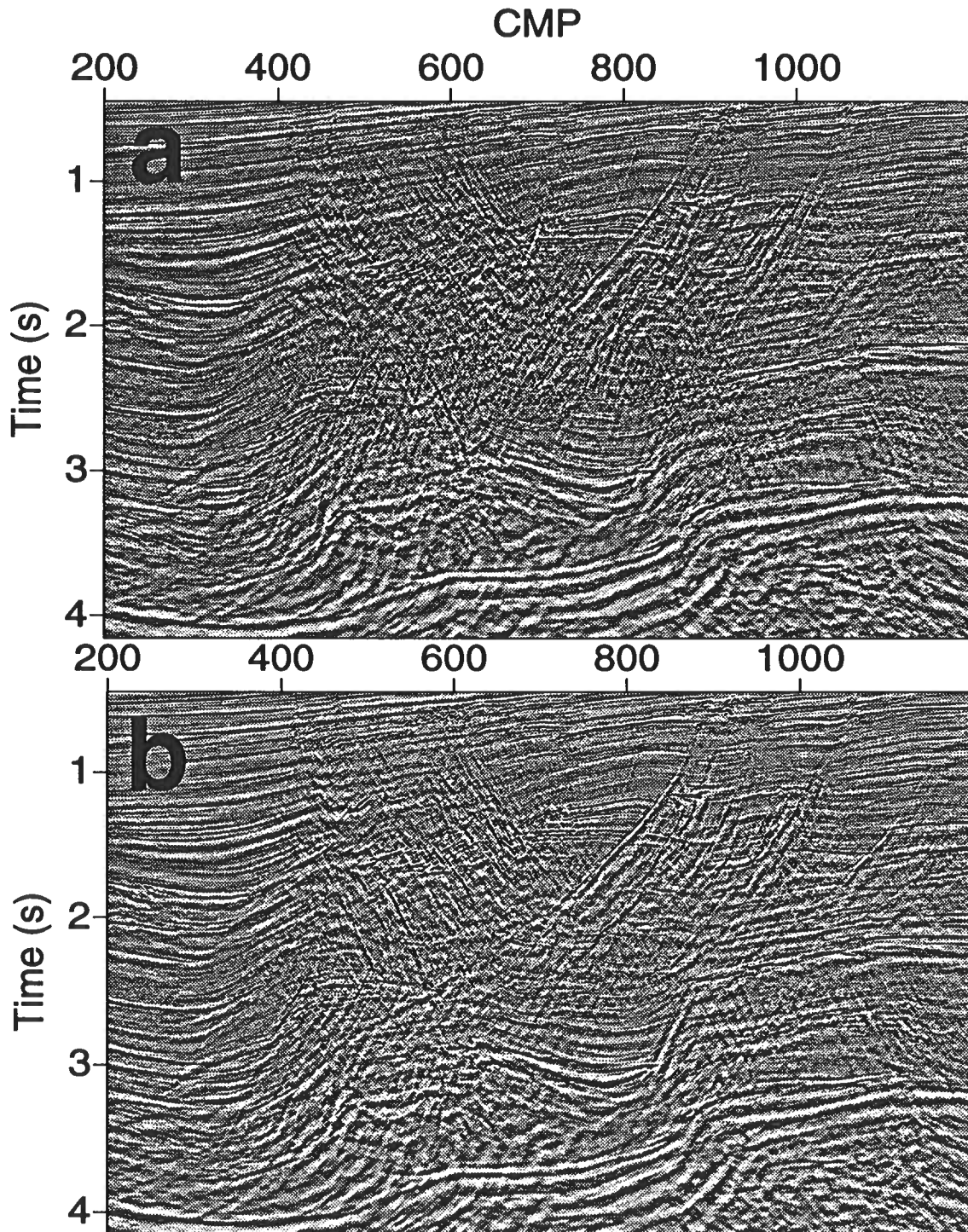


FIG. 9. Time migrated section using (a) isotropic phase-shift migration of the data shown in Figure 4, and (b) anisotropic phase-shift migration of the data shown in Figure 6 using the parameters shown in Figure 5.

overburden on moveout velocity can be stripped through a Dix-type differentiation procedure.

Using sloping reflections to extract velocity information in $v(z)$ media requires, among other things, positioning the reflections at their true (migrated) position. This is accomplished by relating the zero-offset time to the vertical (migrated) time, and therefore positioning the extracted interval velocities at their true times (relative depths). Although this concept is beneficial in isotropic media, it is exceptionally important in anisotropic media, where such velocities are compared with those extracted from horizontal events, and then used to invert for anisotropy information, specifically η . This inversion process is based on the rms assumption of stacking velocities for a given ray parameter. Such a relation, for horizontal reflectors, reduces to the familiar Dix (1955) expression. The idea underlying the inversion is that the $v_{\text{nmo}}(\tau)$ and $\eta(\tau)$ functions obtained from the inversion are those that best focus reflections from the dipping fault and the horizontal reflectors at the same stacking (or NMO) velocity, for each vertical time at which the velocity measurements are made.

Analysis of dip moveout and time-migration impulse responses shows that these processes depend solely on two parameters $v_{\text{nmo}}(0)$ and η in vertically inhomogeneous media. Therefore, the results of the inversion [values of $v_{\text{nmo}}(0)$ and η] can be used to apply NMO, DMO, and time migration. To an extent, time migration can be used to evaluate the performance of the inversion in data that include reflectors with known positions (i.e., fault traces as delimited by terminations of sedimentary bedding). Specifically, the results of the inversion for η can be checked by inspecting the quality of images generated by poststack migration using the same inverted parameters. If the image indicates undermigration, the true η overall is higher than the estimated values.

As we saw in the field example, isotropic DMO cannot properly focus dipping reflectors where the inversion results indicate that the medium is anisotropic. On the other hand, $v(z)$ VTI DMO based on the inverted values of $v_{\text{nmo}}(\tau)$ and $\eta(\tau)$ did focus such reflectors, and, because it also takes non-hyperbolic moveout into account, it can even improve the focussing of horizontal reflections, as well. In addition, anisotropic time migration based on the inverted parameters [$v_{\text{nmo}}(\tau)$ and $\eta(\tau)$] placed the steep reflections at their true time migrated position, while the isotropic migration, which used only the values of $v_{\text{nmo}}(\tau)$, mispositioned the sloping features relative to the horizontal ones.

The cost of anisotropic processing is close to that of its isotropic counterpart. In fact, the processing algorithms needed for both types of media run in about the same time. For example, although slower than the typical log-stretched DMO techniques, the DMO algorithm used here (Alkhalifah, 1995) is as efficient as Artley and Hale's (1994) isotropic $v(z)$ DMO. The difference in computation effort for the isotropic and anisotropic algorithms in phase-shift time migration is negligible. The true additional cost of the anisotropic processing arises from the time needed to measure stacking velocities, as well as ray parameters, for the sloping reflections.

Applying a general anisotropic processing sequence, therefore, is appropriate for all data. If the medium is isotropic, then the lack of anisotropy will be reflected in the small values for the inverted parameter η ($\eta \approx 0$). However, if η departs from zero by a substantial amount (i.e., $\eta > 0.05$), then it is best to take anisotropy into account. Practically, typical performance of isotropic DMO suggests anisotropy in data. In particular, the fact that an isotropic homogeneous DMO works better than isotropic $v(z)$ DMO in a vertically inhomogeneous medium suggests the presence of anisotropy because this anisotropy counters the influence of an increase in velocity with depth. Nevertheless, the fact that isotropic constant-velocity DMO often works better than the $v(z)$ DMO does not imply that the result is optimum. The DMO process can further benefit from an added degree of freedom, in our case η , which can be calculated and has a physical basis, specifically anisotropy. Because it has this physical basis this same parameter provides the added degree of freedom needed in migration as well.

ACKNOWLEDGMENTS

I thank Ken Larner and Ilya Tsvankin for reviewing the manuscript. I also thank my peers Gabriel F. Alvarez and Abdulfattah Al-Dajani for their review of the paper. I wish to thank Tagir Galikeev for loading and preprocessing the data, and John Toldi and Chris Dale of Chevron Overseas Petroleum, Inc. for providing the field data. I also wish to acknowledge the financial support from KACST (Saudi Arabia).

REFERENCES

- Alkhalifah, T., 1995a, Transformation to zero offset in transversely isotropic media: submitted to Geophysics.
- Alkhalifah, T., 1995b, Velocity analysis using nonhyperbolic moveout in transversely isotropic media: Center for Wave Phenomena, Colorado School of Mines (CWP-167).
- Alkhalifah, T., and Larner, K., 1994, Migration errors in transversely isotropic media: Geophysics, **59**, 1405-1418.
- Alkhalifah, T., and Tsvankin, I., 1995, Velocity analysis for transversely isotropic media: Geophysics, in press.
- Artley, C. T., and Hale, D., 1994, Dip moveout processing for depth-variable velocity: Geophysics, **59**, 610-622.
- Byun, B. S., and Corrigan, D., 1990, Seismic traveltimes inversion for transverse isotropy: Geophysics, **55**, 192-200.
- Dix, C. H., 1955, Seismic velocities from surface measurements: Geophysics, **20**, 68-86.
- Gazdag, J., 1978, Wave equation migration with the phase-shift method: Geophysics, **43**, 1342-1351.

- Gonzalez, A., Levin, F. K., Chambers, R. E., and Mobley, E., 1992, Method of correcting 3-D DMO for the effects of wave propagation in an inhomogeneous earth, 62nd Ann. Internat. Mtg., Soc. Expl. Geophys., Expanded Abstracts, 966–969.
- Hake, H., Helbig, K., and Mesdag, C. S., 1984, Three-term Taylor series for $t^2 - x^2$ curves over layered transversely isotropic ground: *Geophys. Prosp.*, **32**, 828-850.
- Hale, D., and Artley, C., 1993, Squeezing dip moveout for depth-variable velocity: *Geophysics*, **58**, 257-264.
- Kitchenside, P. W., 1991, Phase shift-based migration for transverse isotropy, 61st Ann. Internat. Mtg., Soc. Expl. Geophys., Expanded Abstracts, 993-996.
- Lynn, W., Gonzalez, A., and MacKay, S., 1991, Where are the fault-plane reflections?, 61st Ann. Internat. Mtg., Soc. Expl. Geophys., Expanded Abstracts, 1151–1154.
- Sena, A. G., 1991, Seismic traveltimes equations for azimuthally anisotropic and isotropic media: Estimation of internal elastic properties: *Geophysics*, **56**, 2090–2101.
- Thomsen, L., 1986, Weak elastic anisotropy: *Geophysics*, **51**, 1954–1966.
- Tsvankin, I., 1995, Normal moveout from dipping reflectors in anisotropic media: *Geophysics*, **60**, 268-284.
- Tsvankin, I., and Thomsen, L., 1994, Nonhyperbolic reflection moveout in anisotropic media: *Geophysics*, **59**, 1290-1304.
- Tsvankin, I., and Thomsen, L., 1995, Inversion of reflection traveltimes for transverse isotropy: *Geophysics*, in print.

APPENDIX A: VELOCITY ANALYSIS IN LAYERED MEDIA

The first step of the inversion process involves estimating stacking velocities as a function of zero-offset traveltimes from P -wave reflection data. These velocities are commonly considered to equal the NMO velocity. Measuring stacking velocities is common practice in isotropic processing, but here we must estimate such stacking velocities for dipping, as well as horizontal reflections. In addition, we must measure the ray parameters (slopes) corresponding to these reflections.

The inversion method can be applied using any number of dips using a least-squares approach. For simplicity, I constrain the description here to the model given in Figure A-1, where we have only two distinct dips (horizontal reflectors and a dipping fault). The medium is considered to be laterally homogeneous above the fault. Note that, because it is dipping, this single fault provides velocity information at several zero-offset times that can be used to extract vertical parameter variations with depth.

After obtaining stacking-velocity information as a function of ray parameter and zero-offset time, we need to construct an interval-velocity model that satisfies the measured stacking velocities based on equation (6). As mentioned in the text, the

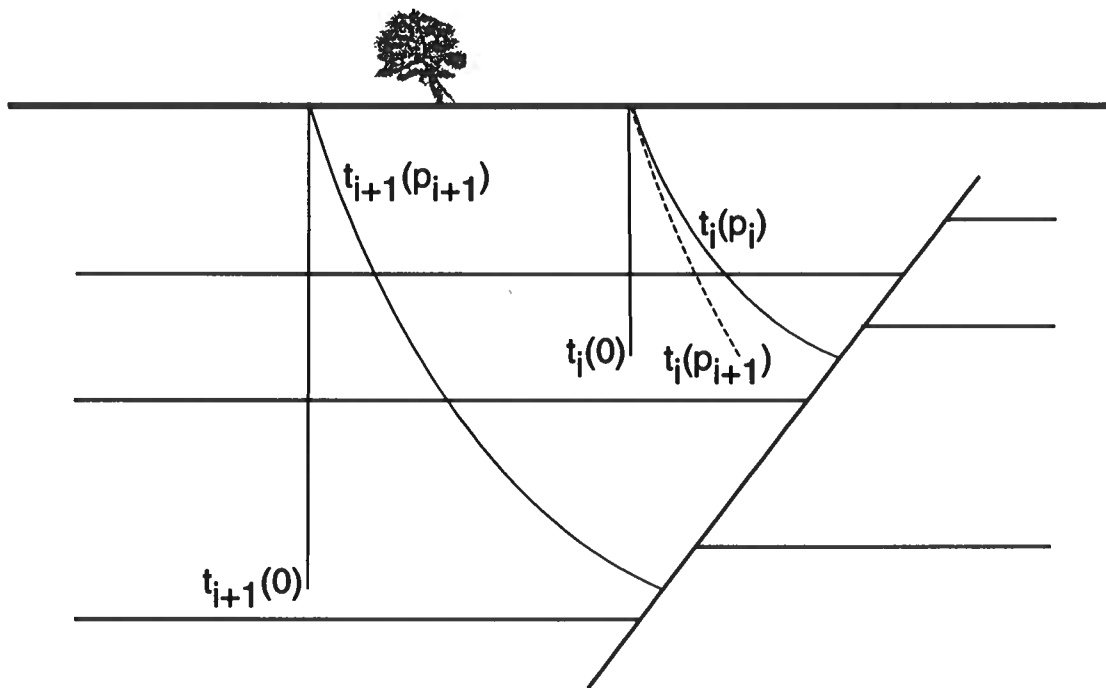


FIG. A-1. Depth model consisting of a fault and a number of horizontal layers. The rays drawn correspond to the measured stacking velocities ($V_{\text{nmo}}[p_i, t_i(p_i)]$ and $V_{\text{nmo}}[p_{i+1}, t_{i+1}(p_{i+1})]$) described in the Appendix. Such rays illustrate the relation between the zero-offset time and the vertical time for the dipping fault.

velocity model that I use is continuous with linear increases in modified interval velocity (a quantity that depends on ray parameter) between the measured values of stacking velocities. For the horizontal reflectors ($p = 0$), construction of such a velocity model is straightforward, following the familiar method of Dix (1955). However, for the dipping fault, the problem is much more complicated because the ray parameter along the fault reflection varies with recording time due to the variation of velocity with depth. Therefore, the measured stacking velocities for the dipping fault at different vertical times correspond to different ray parameters.

Suppose we want to fit a linear interval-velocity model between the measured stacking velocities $V_{\text{nmo}}[p_i, t_i(p_i)]$ and $V_{\text{nmo}}[p_{i+1}, t_{i+1}(p_{i+1})]$, where p_i and t_i are the ray parameter and zero-offset time of the fault reflection used in measuring the stacking velocities. This linear interval velocity will correspond to a ray parameter p_{i+1} and should be continuous with the calculated interval velocities prior to time $t_i(0)$ at this same ray parameter p_{i+1} . Here, $t_i(0)$ is the two-way vertical traveltime to the reflection recorded at time $t_i(p_i)$, as shown in Figure A-1. Therefore, the initial velocity for the linear model between $V_{\text{nmo}}[p_i, t_i(p_i)]$ and $V_{\text{nmo}}[p_{i+1}, t_{i+1}(p_{i+1})]$ is $v_{\text{nmo}}[p_{i+1}, t_i(0)]$ calculated at vertical time $t_i(0)$ using the values of $v_{\text{nmo}}(0, \tau)$ and $\eta(\tau)$ at $\tau = t_i(0)$. The interval values in between the two measured stacking velocities are given by

$$v_{\text{nmo}}(p_{i+1}, \tau) = v_{\text{nmo}}[p_{i+1}, t_i(0)] + a_{i+1}[t(p_{i+1}, \tau) - t_i(p_{i+1})], \quad (\text{A-1})$$

where a_{i+1} is the constant velocity gradient between vertical time $t_i(p_{i+1})$ and $t_{i+1}(p_{i+1})$, and $t(p_{i+1}, \tau)$ is the zero-offset two-way traveltime calculated as follows

$$t(p_{i+1}, \tau) = \int_0^\tau f[\eta(\tau_1), v_{\text{nmo}}(\tau_1), p_{i+1}] d\tau_1, \quad (\text{A-2})$$

where f , as mentioned in the text, is the operator that relates zero-offset time to vertical time. Here, τ corresponds to the two-way vertical time, and $t_i(p_{i+1})$ is the two-way zero-offset traveltime computed, using equation (A-2) by setting $\tau = t_i(0)$. For $i = 0$ (corresponding to the earth's surface), $t_0(p) = 0$, and the interval velocities are estimated either by considering the medium to be homogeneous up to time $t_1(0)$ ($a_1 = 0$), or by using a value for the velocity at the surface that satisfies a certain condition (i.e., for marine data, velocity at the surface is usually set to 1.5 km/s). Therefore, the only unknowns in equation (A-1) as we progress from the top to the bottom of the seismic section are the velocity gradients a_i .

Using the expressions of stacking velocities and traveltimes given above, equation (6) can be written as follows

$$V_{\text{nmo}}^2[p_{i+1}, t_{i+1}(p_{i+1})]t_{i+1}(p_{i+1}) = \int_0^{t_i(p_{i+1})} v_{\text{nmo}}^2(p_{i+1}, \tau) d\tau + \int_{t_i(p_{i+1})}^{t_{i+1}(p_{i+1})} v_{\text{nmo}}^2(p_{i+1}, \tau) d\tau. \quad (\text{A-3})$$

The first term on the right hand side can be calculated from the estimated values of η and $v_{\text{nmo}}(0)$ prior to $t_i(0)$. Let us assume that it equals f_1 . If we are trying to determine a_1 corresponding to the region between the surface and the first measurement, then f_1 equals zero because $t_0(p_{i+1})=0$.

Substituting equation (A-1) into the second term of equation (A-3) results in a quadratic equation in a_{i+1} . Solving equation (A-3) for a_{i+1} involves solving the quadratic equation, and therefore

$$a_{i+1} = 0.5 \left(\sqrt{\frac{4V_{\text{nmo}}^2[p_{i+1}, t_{i+1}(p_{i+1})]t_{i+1}(p_{i+1}) - v_{\text{nmo}}^2[p_{i+1}, t_i(p_{i+1})]t_d}{t_d^2} - 4f_1} - \frac{v_{\text{nmo}}^2[p_{i+1}, t_i(p_{i+1})]}{t_d} \right),$$

where $t_d = t_{i+1}(p_{i+1}) - t_i(p_{i+1})$.

Each time a new velocity gradient is obtained, for example a_{i+1} , it is directly used to compute the interval velocities using equation (A-1) in the region between $t_i(0)$ and $t_{i+1}(0)$. Then, these interval velocities, which correspond to the dipping fault, along with the horizontal interval NMO velocities, are used to invert — one sample at time — for $v_{\text{nmo}}(0, \tau)$ and $\eta(\tau)$ based on the homogeneous DMO inversion of Alkhalifah and Tsvankin (1995). We continue to invert for $v_{\text{nmo}}(0, \tau)$ and $\eta(\tau)$ as a function of vertical time until we reach the time $t_{i+1}(0)$. Then a new velocity gradient, a_{i+2} , for the region between $t_{i+1}(0)$ and $t_{i+2}(0)$ is calculated in the same way.